



Published in final edited form as:

Bioorg Med Chem Lett. 2017 March 01; 27(5): 1252–1255. doi:10.1016/j.bmcl.2017.01.059.

Bidentate iminodiacetate modified dendrimer for bone imaging

Lara Pes^{a,†}, Young Kim^{a,b,†}, and Ching-Hsuan Tung^{a,*}

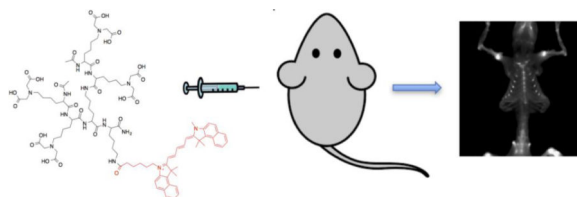
^aMolecular Imaging Innovations Institute, Department of Radiology, Weill Cornell Medicine, New York, NY, 10021, USA

^bDepartment of Pathology, Chonnam National University Medical School, 671, Jebongno, Dong-Gu, Gwangju, 501-757 Korea

Abstract

A new dendrimer probe was designed for bone imaging. Bidentate iminodiacetate groups were introduced to the probe to obtain strong bind to bones. The assembled dendrimeric probe, with four iminodiacetate moieties and a fluorescent tag, displayed good selectivity to hydroxyapatite, calcium oxalate and calcium phosphate salts. In mice, the probe offered vivid skeletal details after intravenous delivery.

Graphical Abstract



Keywords

bone; fluorescence imaging; hydroxyapatite; iminodiacetate; dendrimer

Bones represent over 99% of the calcium deposits in the human body. With the exception of teeth and pathological calcifications, bones differ from other body tissues in their unique calcium mineral composition, which consists mainly of hydroxyapatite (HA). Because of this characteristic, molecules that recognize HA could be used to deliver drugs or imaging agents for the treatment and diagnosis of bone diseases.

*Correspondence to: Ching H. Tung, Weill Cornell Medical College, 413 East 69th Street, Box 290, New York, NY 10021. cht2018@med.cornell.edu.

†These authors contributed equally to the project.

Publisher's Disclaimer: This is a PDF file of an unedited manuscript that has been accepted for publication. As a service to our customers we are providing this early version of the manuscript. The manuscript will undergo copyediting, typesetting, and review of the resulting proof before it is published in its final citable form. Please note that during the production process errors may be discovered which could affect the content, and all legal disclaimers that apply to the journal pertain.

Supplementary Material

Supplementary data associated with this article can be found, in the online version, at

Bisphosphonates (Figure 1) are the most widely used class of compounds for the selective binding of HA and, because of their ability to interfere with the activity of osteoclasts, they are effective in the treatment of osteoporosis, Paget's disease, and malignant hypercalcemia.^{1, 2} Bisphosphonates are analogs of the natural bone-binding molecule pyrophosphate, where the oxygen between two phosphates is replaced with a carbon atom. This achieves a better stability against biological degradation without losing its ability to chelate the calcium in the hydroxyapatite of bones.³⁻⁵

Bisphosphonates have been widely exploited not only to deliver therapeutic agents to the bones, but also for medical diagnoses when they are chelated to a radiotracer. An example is ^{99m}Tc-methylene diphosphonate (MDP), which detects metastatic bone cancer, Paget's disease and osteoporotic fractures via bone scintigraphy.⁵ Near-infrared fluorescent dyes can be conjugated to the bisphosphonates as an alternative to radioisotopes in pre-clinical studies.⁶ Though bisphosphonate is an excellent bone targeting agent, it causes side effects, such as osteonecrosis.⁷ Non-bisphosphonate based bone homing agents thus have also been explored.

Peptide-based molecules are the second major category of bone targeting ligands, and most of them are derived from natural bone binding proteins.⁸⁻¹¹ These peptides all contain an unusually high density of acidic amino acid residues. Poly-glutamate (poly-Glu) and poly-aspartate (poly-Asp) peptides, for example, have been used for bone targeting.^{5, 12, 13} These peptides chelate calcium salt through multiple carboxylates present on the side chain of amino acids. Recently, a (AspSerSer)₆ polypeptide that transports an siRNA containing liposome to bone was reported.¹⁴ Although several acidic peptides for bone delivery have been documented, their affinity is suboptimal.

Osteocalcin is a protein that is produced by the osteoblasts, and involved in bone formation and healing. Osteocalcin binds to HA through a region with three γ -carboxy-glutamic acid (Gla) residues (Figure 1). Gla is an unusual amino acid that is derived from glutamic acid through the addition of a second carboxylic acid functional group on the side chain via the vitamin K-dependent γ -carboxylation.¹⁵ Previously a 19-mer peptide, called HBP-19, that incorporated six residues of Gla was developed by us and showed excellent properties as a bone imaging probe both in vitro and in vivo.⁹ In that study, it was found that the peptide lost its affinity to HA if the unusual bidentate Gla residues were replaced by normal Glutamate (Glu) residues (Figure 1), which have only one carboxyl group on the side chain, suggesting the critical role of the bidentate structure. An iminodiacetate (IDA) group (Figure 1), which imitates the bidentate structure of dicarboxylate group on the Gla side chain, has been explored for bone binding. Dendritic tetra-iminodiacetate moieties were used to deliver a deep-red fluorescent probe¹⁰ and an iodine rich computer tomography (CT) contrast agent.¹⁶ Preclinical animal studies have shown that a multi (more than two) IDA moiety, could be applied to target bones.^{10, 17} In addition, the study also indicated that the distance between the carboxylic acid and the nitrogen in the chelating moiety is critical in HA binding.¹⁰ It was reported that one-carbon spacer (i.e. IDA, iminodiacetate) was significantly better than a two-carbon spacer (i.e. iminodipropionate).

These findings led us to develop a simple bone-targeting domain with a flexible modularity. Our approach was to reduce the size of the structure and the number of negatively charged residues that could complicate purification, by moving towards a dendritic arrangement via a simple coupling reaction. A simple fluorescent bone-imaging agent, termed iminodiacetate-modified poly-L-lysine dendrimer (IMPLD, 9), was synthesized using a convergent approach (Scheme 1). To avoid the use of costly Glu residues for HA chelation, a fully protected di-IDA containing a di-lysine block (5) was obtained through a nucleophilic substitution of tert-butyl bromoacetate (4) to the ϵ -amino groups of the α -acetylated Lys dimer (3, Figure S1). The preparation of the solution for this fully protected di-IDA block (5) has made the synthesis of IMPLD straightforward. The core di-lysine peptide (6) was prepared on a Rink amide resin with Fmoc-Lys (ivDde) and Fmoc-Lys(Fmoc) residues, following the standard solid phase synthesis. The two Fmoc protecting groups were simultaneously removed on the resin to react with the di-IDA block (5). Thereafter, the removal of the ivDde group led to a free ϵ -amino group on the C-terminal lysine side chain (7). This was used for the subsequent conjugation with a reporter or compound of interest. In this study, two fluorescent tags, fluorescein and cyanine 5.5 (Fig S2), were conveniently attached to demonstrate their usages. The prepared IMPLD was purified by HPLC and characterized by Mass spectrometry and NMR. (Supplementary information)

An alternate divergent synthetic approach was also investigated. The IDA-modified lysines were first synthesized from Fmoc-L-lysine and tert-butyl bromoacetate and then added step by step onto the core on the solid support. However, this strategy was found to be inefficient and led to low yields and difficult purification (data not shown). Peptide dendrimers are known to be difficult to purify and characterize,¹⁸ especially when the divergent approach is followed.¹⁹ The current convergent synthesis is preferred to the divergent because it allows for a second purification step before coupling the di-IDA block (5) to the core (6). This second purification makes the final purification easier and more effective; despite the incomplete coupling side-products that were still detected. These impurities are believed to be due to the steric hindrance of the dendritic structure that impedes the complete coupling of the side chains to the core.

The purified IMPLD with a fluorescein tag (9) was tested in vitro for its ability to bind biologically relevant calcium salts. Five major calcium salts found in the human body are HA, calcium oxalate (CaOx), calcium carbonate (CaCO₃), calcium phosphate (Ph), and calcium pyrophosphate (Py). HA is the main component in bones and teeth. It is also found in atherosclerotic plaques and osteotropic tumors, such as breast and prostate cancers.^{20, 21} CaOx is present in tumors as well, but contrary to HA, it is found mostly in benign tumors.^{21, 22} CaOx, together with calcium phosphate, is also the main component of nephrolithiasis.^{23–25} Py is deposited in the joints in pathological conditions such as pseudogout.²⁶

After incubating the fluorescein label IMPLD (10 μ M) with the salts for 3 hours, the supernatants were collected and their absorbance was compared to the original solution. The reduction in the absorbance was interpreted as the binding of the IMPLD molecules to the surface of the salts. A lower absorbance, therefore, corresponds to a higher affinity of IMPLD for the salt. The results were reported as a percentage of binding (Figure 2a). The

best bindings were obtained for CaOx, Ph, and HA with 93%, 77% and 61%, respectively, while IMPLD bound poorly to CaCO₃ and Py. The binding of IMPLD can be visualized on the precipitated salts with the naked eye (Figure 2c) and looking at the difference in the fluorescence of the supernatant (Figure 2b).

It is encouraging to find that IMPLD, with four external bidentate IDA groups, is sufficient to achieve high HA binding. Based on its affinity to HA, IMPLD could be used as a bone homing ligand. In order to prove this potential in vivo, fluorescein was replaced with a more suitable near-infrared fluorescent dye, cyanine 5.5 (Cy5.5-IMPLD, Fig S2), and was conjugated to IMPLD using the same method.

After the intravenous injection of Cy5.5-IMPLD (20 nmol), the anterior images showed an immediate whole body distribution and a fast kidney elimination of the probe (Fig 3a). A high fluorescence signal was seen in the bladder at 3 and 6 hours post injection. The fluorescence signal started to appear in the bones within hours and was retained for weeks. A further clearance of the background signal made the bone signal more apparent. For example, at day 4, a strong signal was clearly seen in the knees and rib cage. The contrast ratio of bone to muscle continued to increase until 2 weeks. The maximum contrast was ~ 5 folds above the background, and the signal was sustained for more than 4 weeks in vivo (Fig 3b). Dorsal images also showed a high initial accumulation of the probe within the kidney (Figure S3, Supplementary information). The ex vivo image of the excised organs further confirmed the initial accumulation of the probes in the kidney and liver at day 1, while the probe was completely cleared from most organs 2 weeks later (Figure S4, Supplementary information). Fluorescence imaging was conducted ex vivo after the skin was removed. Without the interference of the skin, the ex vivo fluorescence images showed remarkable details of the bone structures, such as the sternum, vertebra, rib cage, femur and tail (Figure 3c), indicating that IMPLD did have a good affinity to bone. Its safety was then validated by incubating IMPLD (0.1 – 50 μM) with NIH3T3 fibroblasts, and the MTS cytotoxicity assay confirmed that IMPLD is not toxicity at this range (Fig S5).

The in vivo image study of the fluorescently labeled IMPLD showed preferential bone accumulation. Although all bones could be labeled, the highest signal was observed in bones located near growth plates, such as the femoral heads, lumbar vertebrae, and scapulae. Previously, we have used the osteocalcin mimic HABP-19 to demonstrate that the HA binding probes are useful not only for bone images but also for the diagnosis of pathological calcifications such as breast and arterial calcifications, which could be a sign of breast cancer²¹ and atherosclerosis,²⁷ respectively. It is rational to postulate that IMPLD might have similar medical potential. Compared to HABP-19, IMPLD has though the advantage of an easier preparation.

Herein the in vitro characterization and in vivo validation preparations of a new tetra-IDA containing IMPLD are described. IMPLD exploits bidentate IDA groups for HA binding. This non-bisphosphonate bone homing agent could find an application in the diagnosis of orthopedic diseases, such as osteoporosis and hyperostosis, as well as arterial calcifications or decalcifications. IMPLD's modularity, allows for the possibility of replacing the fluorophore with chelators for radioisotopes. With further structural modifications to achieve

the appropriate pharmacokinetics, IMPLD could be a valuable lead compound for various imaging techniques, such as PET and SPECT. IMPLD also showed an efficient binding to CaOx and HA, found in osteotropic tumors. This allows IMPLD to be employed in the diagnosis of these tumors, or to be used as targeting ligand for the delivery of chemotherapy drugs or therapeutic agents. IDA functionalization could be used as a general approach to bone targeting by increasing affinity for HA, enabling the transport of other molecules or particles to bones.

Supplementary Material

Refer to Web version on PubMed Central for supplementary material.

Acknowledgments

This study was financially supported in part by NIH GM094880. The authors would like to thank the Nuclear Magnetic Resonance Core facility at Weill Cornell Medical College.

References and notes

1. Zhang S, Gangal G, Uludag H. *Chem. Soc. Rev.* 2007; 36:507–531. [PubMed: 17325789]
2. Russell RG, Watts NB, Ebetino FH, Rogers MJ. *Osteoporos Int.* 2008; 19:733–759. [PubMed: 18214569]
3. Rodan GA, Martin TJ. *Science.* 2000; 289:1508–1514. [PubMed: 10968781]
4. Low SA, Kopecek J. *Adv Drug. Deliv. Rev.* 2012; 64:1189–1204. [PubMed: 22316530]
5. Ogawa K, Ishizaki A, Takai K, Kitamura Y, Kiwada T, Shiba K, Odani A. *PLoS One.* 2013; 8:e84335. [PubMed: 24391942]
6. Zaheer A, Lenkinski RE, Mahmood A, Jones AG, Cantley LC, Frangioni JV. *Nat. Biotechnol.* 2001; 19:1148–1154. [PubMed: 11731784]
7. Khosla S, Burr D, Cauley J, Dempster DW, Ebeling PR, Felsenberg D, Gagel RF, Gilsanz V, Guise T, Koka S, McCauley LK, McGowan J, McKee MD, Mohla S, Pendrys DG, Raisz LG, Ruggiero SL, Shafer DM, Shum L, Silverman SL, Van Poznak CH, Watts N, Woo SB, Shane E. *J. Bone Miner. Res.* 2007; 22:1479–1491. [PubMed: 17663640]
8. Yarbrough DK, Hagerman E, Eckert R, He J, Choi H, Cao N, Le K, Hedger J, Qi F, Anderson M, Rutherford B, Wu B, Tetradis S, Shi W. *Calcif. Tissue Int.* 2010; 86:58–66. [PubMed: 19949943]
9. Lee JS, Tung CH. *Chembiochem.* 2011; 12:1669–1673. [PubMed: 21661088]
10. Brounts SH, Lee JS, Weinberg S, Lan Levengood SK, Smith EL, Murphy WL. *Mol. Pharm.* 2013; 10:2086–2090. [PubMed: 23506396]
11. Gilbert M, Shaw WJ, Long JR, Nelson K, Drobny GP, Giachelli CM, Stayton PS. *J. Biol. Chem.* 2000; 275:16213–16218. [PubMed: 10748043]
12. Fujisawa R, Wada Y, Nodasaka Y, Kuboki Y. *Biochim. Biophys. Acta.* 1996; 1292:53–60. [PubMed: 8547349]
13. Sekido T, Sakura N, Higashi Y, Miya K, Nitta Y, Nomura M, Sawanishi H, Morito K, Masamune Y, Kasugai S, Yokogawa K, Miyamoto K. *J. Drug Target.* 2001; 9:111–121. [PubMed: 11697106]
14. Zhang G, Guo B, Wu H, Tang T, Zhang BT, Zheng L, He Y, Yang Z, Pan X, Chow H, To K, Li Y, Li D, Wang X, Wang Y, Lee K, Hou Z, Dong N, Li G, Leung K, Hung L, He F, Zhang L, Qin L. *Nat. Med.* 2012; 18:307–314. [PubMed: 22286306]
15. Hoang QQ, Sicheri F, Howard AJ, Yang DS. *Nature.* 2003; 425:977–980. [PubMed: 14586470]
16. Parkesh R, Gowin W, Lee TC, Gunnlaugsson T. *Org. Biomol. Chem.* 2006; 4:3611–3617. [PubMed: 16990936]
17. Peck EM, Battles PM, Rice DR, Roland FM, Norquest KA, Smith BD. *Bioconjug. Chem.* 2016; 27:1400–1410. [PubMed: 27088305]

18. Sanclimens G, Crespo L, Giralt E, Royo M, Albericio F. *Biopolymers*. 2004; 76:283–297. [PubMed: 15386270]
19. Sadler K, Tam JP. *Rev. Mol. Biotechnol.* 2002; 90:195–229.
20. Zaheer A, Murshed M, De Grand AM, Morgan TG, Karsenty G, Frangioni JV. *Arterioscler. Thromb. Vasc. Biol.* 2006; 26:1132–1136. [PubMed: 16484598]
21. Lee JS, Tung CH. *Biochim. Biophys. Acta.* 2013; 1830:4621–4627. [PubMed: 23688398]
22. Morgan MP, Cooke MM, McCarthy GM. *J. Mammary Gland Biol. Neoplasia.* 2005; 10:181–187. [PubMed: 16025224]
23. Aggarwal KP, Narula S, Kakkar M, Tandon C. *Biomed. Res. Int.* 2013; 415:292953.
24. Goldfarb DS. *Clin. J. Am. Soc. Nephrol.* 2012; 7:1172–1178. [PubMed: 22595827]
25. Figueiredo JL, Passerotti CC, Sponholtz T, Nguyen HT, Weissleder R. *J. Urol.* 2008; 179:1610–1614. [PubMed: 18295253]
26. Macmullan P, McCarthy G. *Ther Adv Musculoskelet Dis.* 2012; 4:121–131. [PubMed: 22870500]
27. Lee JS, Morrisett JD, Tung CH. *Atherosclerosis.* 2012; 224:340–347. [PubMed: 22877867]

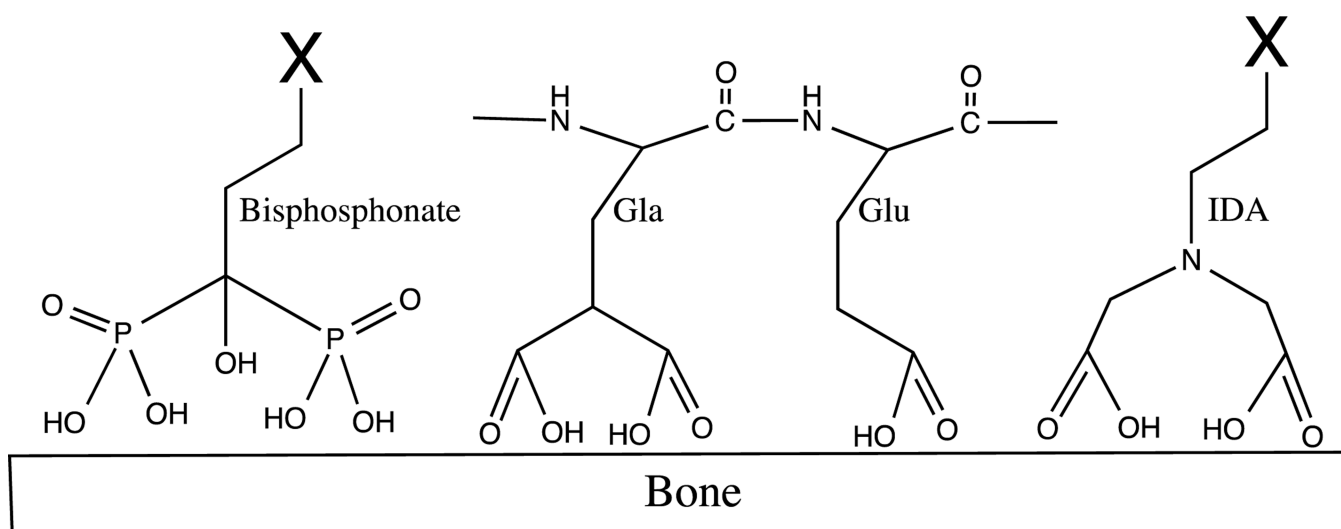


Figure 1.
Schematic structure of bisphosphonates, γ -carboxy-glutamic acid (Gla), glutamate (Glu) and iminodiacetate (IDA)

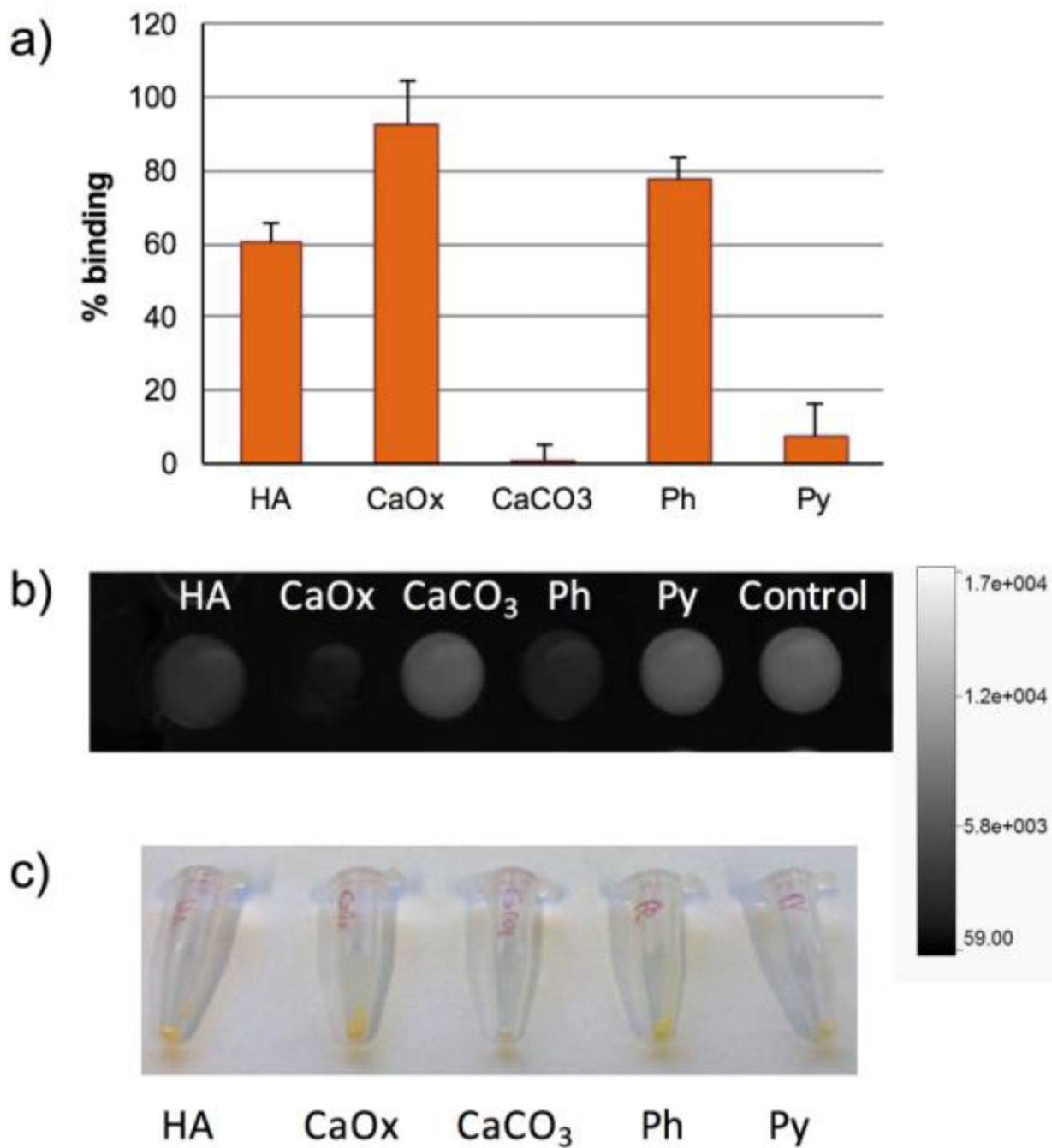


Figure 2. Comparison of IMPLD binding to calcium salts. IMPLD in TRIS buffer (100 μ L, 10 μ M) were incubated for 3 h with 2.5 mg of HA, CaOx, CaCO₃, Ph and Py. (a) Percentage of binding of IMPLD; (b) fluorescence intensity of the supernatant of IMPLD after 3 h incubation with the salts; (c) photo of the salts treated with IMPLD after washing.

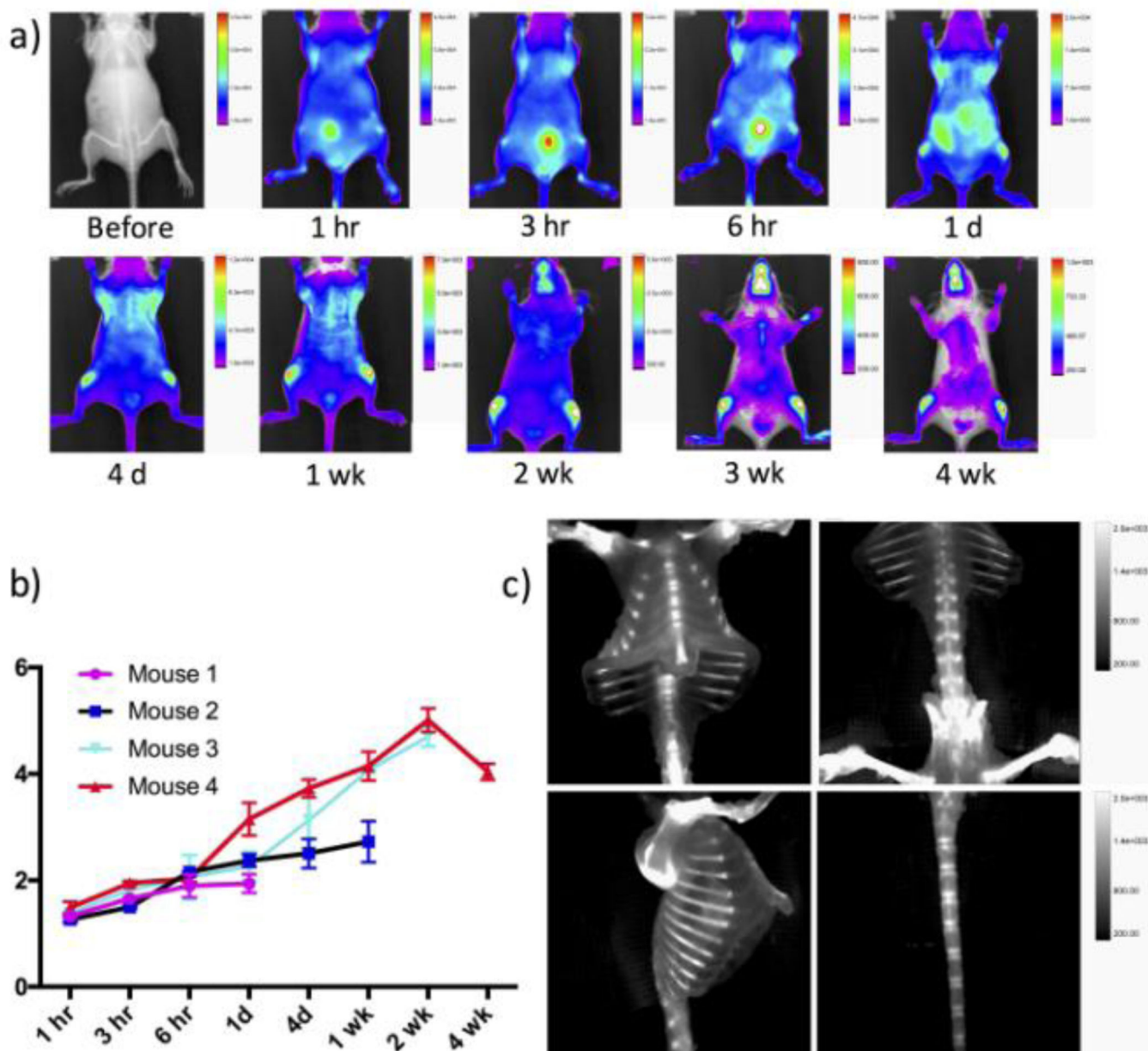
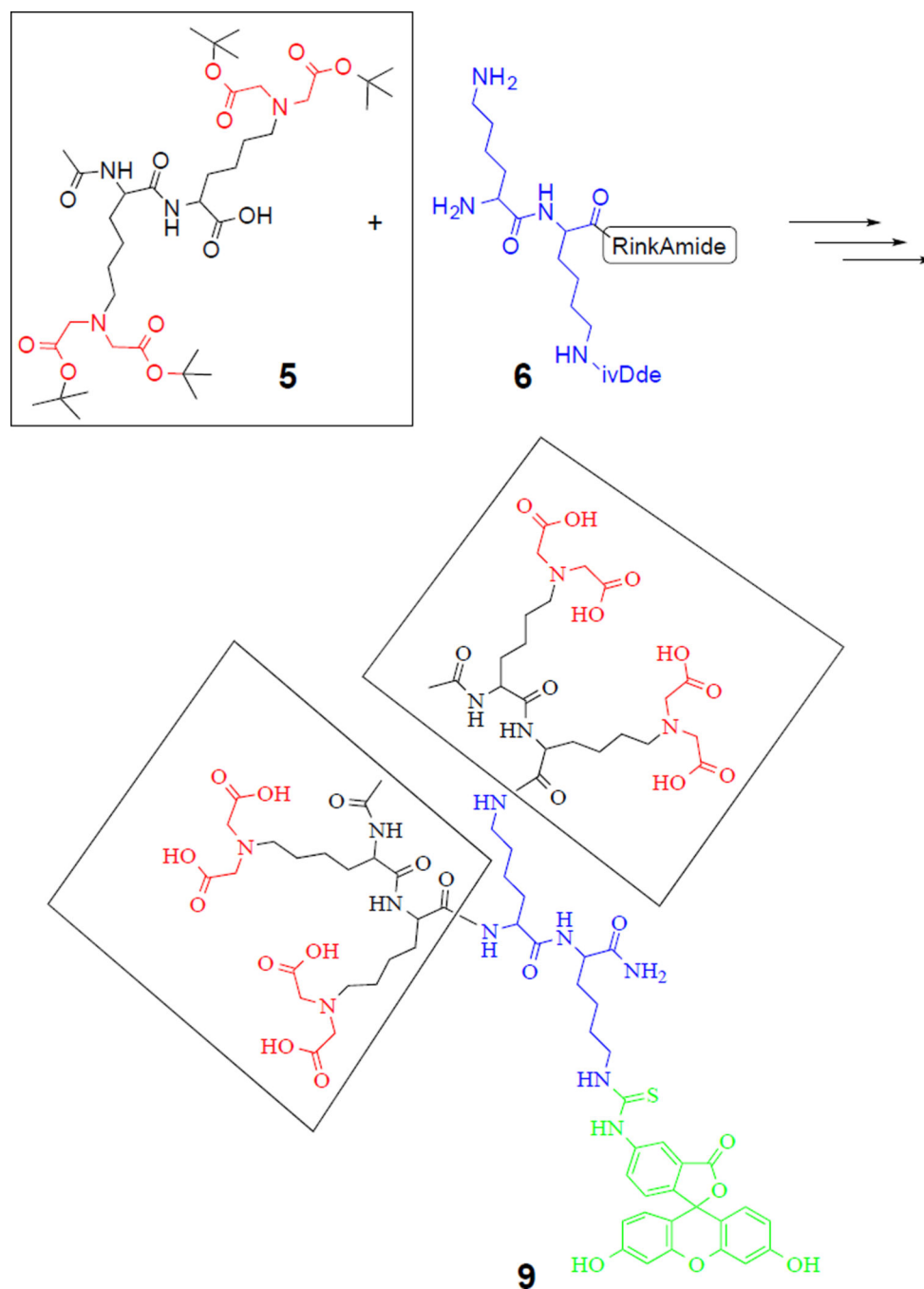


Figure 3.

In vivo and ex vivo fluorescence images post injection of IMPLD. The time dependent images were obtained after injection of 20 nmol of IMPLD with PBS intravenously. (a) In vivo optical images of anterior view at the indicated time points. The fluorescence of marked areas in knees and thigh muscle were measured.; (b) contrast ratios between mean fluorescent intensity of knee and that of thigh muscle at different time points; (c) ex vivo images at week 2 post injection of IMPLD showed the clear fluorescent signal in the various bones.

**Scheme 1.**

Convergent synthesis of IMPLD (9) by coupling two di-lysine(IDA) blocks (5) to a di-lysine core (6) on a solid support.